7

Robust Extraction Interface for Coupling Droplet-Based and Continuous Flow Microfluidics

Xuefei Sun[1], Keqi Tang[1], Richard D. Smith[1,2] and Ryan T. Kelly[2,*]
[1]*Biological Sciences Division*
[2]*Environmental Molecular Sciences LaboratoryPacific Northwest National Laboratory*
USA

1. Introduction

Microdroplets, in which aqueous samples are encapsulated in an immiscible phase (e.g., oil), can serve as microreactors and as vehicles for high-throughput chemical and biological studies. The oil phase separating the small (femto – nanoliter) aqueous volumes serves to eliminate dispersion, sample loss, dilution and cross-contamination. Droplet-based microfluidics also offers great promise for quantitative analysis because monodisperse microdroplets can be generated with controllable sizes and detected at well defined time points. Such platforms have been successfully applied in a number of biological research areas, for example, encapsulating and sorting single cells within droplets, studying enzyme kinetics, and performing polymerase chain reaction (PCR) with high throughput (Chiu & Lorenz, 2009; Chiu et al., 2009; Huebner et al., 2008; Song et al., 2006; Teh et al., 2008; Theberge et al., 2010; Yang et al., 2010).

A variety of methods have been developed to generate, manipulate and monitor droplets in microfluidic devices (Theberge et al., 2010). Detection of droplet contents has historically been limited to optical methods such as laser-induced fluorescence, while coupling with chemical separations and nonoptical detection has proven difficult. Combining the advantages of droplet-based platforms with more information-rich analytical techniques including liquid chromatography, capillary electrophoresis and mass spectrometry (MS) will greatly extend their reach. For example, electrospray ionization (ESI)-MS has become an essential technique for biological analysis because of its high sensitivity and ability to identify and provide structural information for hundreds or more molecules from complex samples in a given analysis (Aebersold & Mann, 2003; Liu et al., 2007). A number of techniques have been developed to couple continuous-flow microfluidic devices with MS (Kelly et al., 2008; Koster & Verpoorte, 2007; Mellors et al., 2008; Sun et al., 2011b), but the coupling of droplet-based platforms with MS remains challenging (Fidalgo et al., 2009).

ESI-MS analysis of aqueous droplets has been achieved by directly coupling a segmented flow system with MS (Pei et al., 2009), but this method has some potential risks including

* Corresponding Author

instability of the electrospray due to oil accumulation at the tip, introduction of chemical background, and contamination of the MS instrument. Hence, it is generally necessary to extract the aqueous droplet from the oil phase for further separation or MS analysis. Huck and coworkers employed electrocoalescence to extract droplets (Fidalgo et al., 2008) in which a pulsed electric field was applied over the extraction chamber to force droplets to coalesce with an aqueous stream. The droplet contents were then delivered to a capillary emitter for ESI-MS detection (Fidalgo et al., 2009). This method required careful adjustments to the flow of two immiscible phases to maintain an interface in the extraction chamber and avoid cross-contamination of the aqueous and oil streams. In addition, the severe dilution of the droplet contents resulted in high (~500 μM) detection limits. Lin and coworkers utilized an electrical-based method to control the droplet disruption and extraction at a stable oil/water interface (Zeng et al., 2011), but one reported issue in this case was the difficulty of achieving complete extraction with high efficiency, which limited its compatibility with quantitative analysis.

Another droplet extraction technique is based on surface modification at the junction between two immiscible phases in the microchannel. Kennedy and coworkers exploited selectively patterned glass microchannel surfaces to stabilize the oil-water interface and facilitate droplet extraction (Pei et al., 2010; Roman et al., 2008; Wang et al., 2009). When the segmented flow matched the aqueous flow, the entire plug was able to be extracted. In some cases only part of each droplet was transferred due to the presence of a "virtual wall" (Pei et al., 2010; Roman et al., 2008). A portion of the extracted samples were then injected into an electrophoresis channel for CE separation. Recently, Fang and coworkers employed a similar surface modification technique to obtain a hydrophilic tongue-based droplet extraction interface, which could control the droplet extraction by regulating the waste reservoir height (Zhu & Fang, 2010). The droplet contents were then detected by MS through an integrated ESI emitter. However, with a height of zero, the droplets were not extracted and aqueous buffer was occasionally transferred to the droplets. In our laboratory, a novel droplet extraction interface constructed with an array of cylindrical posts was developed (Kelly et al., 2009). When the aqueous stream and oil carrier phase flow rates were adjusted to balance the pressure at the junction, a stable oil-aqueous interface based on interfacial tension alone was formed to prevent bulk crossover of two immiscible streams, while the droplets could be transferred through the apertures between posts to the aqueous stream and finally detected by ESI-MS with virtually no dilution.

Most of the reported methods and techniques for droplet extraction, as mentioned above, need to adjust two immiscible liquid flow rates to stabilize the interface and extract entire droplets. It is desirable to perform effective and complete droplet extraction independent of the flow rates, which would provide added flexibility for device operation. In this work, we present a robust interface for reliable and efficient droplet extraction, which was integrated in a droplet-based PDMS microfluidic assembly. The droplet extraction interface consisted of an array of cylindrical posts, the same as was previously reported (Kelly et al., 2009), but the aqueous stream microchannel surface was selectively treated by corona discharge to be hydrophilic. The combination of different surface energies and small apertures (~3 μm × 25 μm) enabled a very stable liquid interface between two immiscible steams to be established over a broad range of aqueous and oil flow rates. All aqueous droplets were entirely transferred to the aqueous stream and detected by MS following ionization at a monolithically integrated electrospray emitter.

2. Experimental section

2.1 Materials

Fluorinert FC-40, leucine enkephalin, apomyoglobin, glacial acetic acid, sodium carbonate, sodium bicarbonate, and hexamethyldisilazane (HMDS) were purchased from Sigma-Aldrich (St. Louis, MO). Fluorescein was obtained from Fluka (Buchs, Switzerland). HPLC-grade methanol was purchased from Fisher Scientific (Fair Lawn, NJ). Water was purified using a Barnstead Nanopure Infinity system (Dubuque, IA). ESI buffer solution was prepared by mixing water and methanol at a 9:1 (v/v) ratio and adding 0.1% (v/v) acetic acid. Carbonate buffer (10 mM, pH 9.3) was filtered using 0.2 μm syringe filters (Pall Life Sciences, Ann Arbor, MI) before use. PDMS elastomer base and curing agent were purchased as Dow Corning Sylgard 184 from Ellsworth Adhesives (Germantown, WI).

2.2 Microfluidic design and fabrication

Figure 1A shows the pattern of an integrated droplet-based microfluidic device that was designed using IntelliCAD software (IntelliCAD Technology Consortium, Portland, OR). It is composed of two-layers, in which the control layer contains two microchannels used for valving, and the flow layer includes all other microchannels and microstructures. Droplet generation is controlled by pneumatic valves (Galas et al., 2009; Sun et al., 2011a; Zeng et al., 2009). The valving intersectional area is 100 μm × 100 μm. The length of the two side channels and the distance between them are 0.5 cm and 100 μm, respectively. The design of the droplet extraction interface is expanded in Figure 1B, which is constructed with an array of 15-μm-diameter cylindrical posts having ~3 μm apertures for fluid transfer in between. The width of both microchannels separated by the interface is 50 μm. The oil flow channel width tapers from 100 μm to 50 μm, ensuring that the droplets can contact the interface sufficiently to enable extraction. Pairs of patterned symmetrical lines with an angle of 50° are used to guide the cutting of a tapered emitter at the aqueous channel terminus (Kelly et al., 2009).

The integrated droplet-based PDMS microfluidic device was fabricated using well established multilayer soft lithography techniques (Sun et al., 2011a; Unger et al., 2000). First, two separate templates were produced on silicon substrates with a contact photomask aligner (NXQ4000-6, Neutronix-Quintel, Morgan Hill, CA). Three photomasks were printed with 50,800 dpi resolution at Fineline Imaging (Colorado Springs, CO) based on the design shown in Figure 1A. The template defining the valving control channels was formed by patterning SU-8 photoresist (Microchem, Newton, MA) with rectangular features (~ 25 μm high). The other template containing the flow layer was fabricated through two steps. Two side channels for injection of dispersed aqueous samples were first patterned with SPR 220-7 photoresist (Rohm & Haas Electronic Materials, Marlborough, MA), which was reflowed to provide rounded shape features (~ 10 μm high) and stabilized at high temperature (180 ^{o}C) for 30 min to prevent removal in subsequent processing steps. The remaining microstructures on the flow layer containing the extraction interface (Figure 1C) were then aligned with the two pregenerated side channels and patterned with SU-8 photoresist to form rectangular shaped features (~25 μm high). The silicon template defining the control layer was modified with HMDS using vapor deposition to assist in releasing the PDMS membrane from the patterned template. A 10:1 ratio (w/w) of PDMS base to curing agent

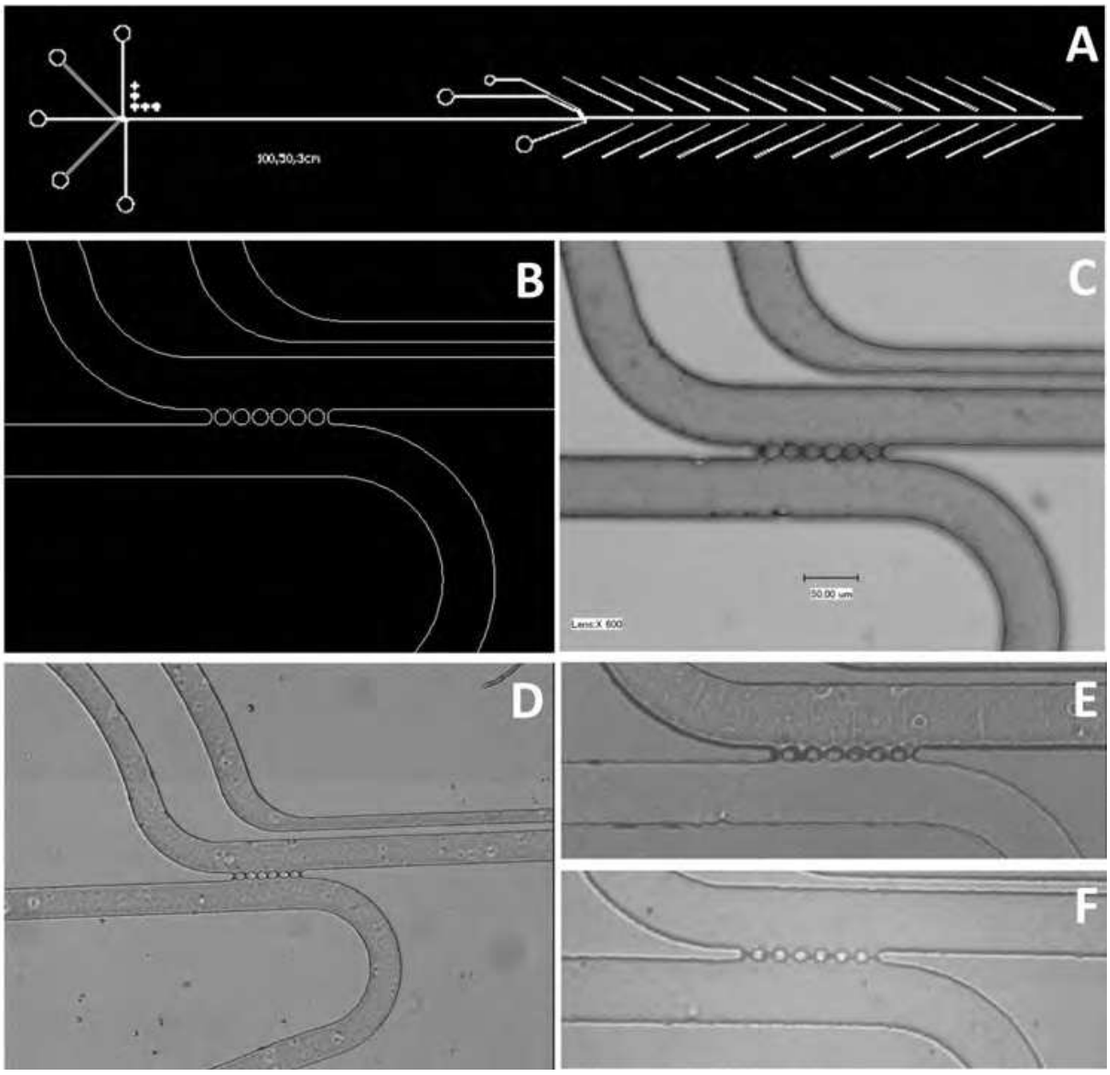

Fig. 1. Overview of device design and fabrication. (A) Design of a droplet-based microfluidic device including a valve-based droplet generator, a droplet extraction interface, and guide marks for cutting the ESI emitter. (B) Amplified view of the droplet extraction interface design. (C) Photograph of the extraction interface structure on a silicon template. (D) Photograph of the extraction interface in a completed PDMS device. (E) Photograph of the water-air interface. Top channel was empty and bottom channel filled with DI water. (F) Photograph of the oil-water interface. Top channel filled with DI water and bottom channel filled with oil (FC-40).

was then mixed, degassed under vacuum, and poured onto the patterned flow layer template to a thickness of 1–2 mm. This PDMS prepolymer mixture was also spin-coated on the HMDS-treated template at 2000 rpm for 30 s to create a control layer membrane with a thickness of ~ 50 µm. Both substrates were cured in an oven at 75 °C for at least 2 h. After removing the patterned PDMS from the flow layer template, several small through-holes were created at the ends of all flow channels by punching the substrate with a manually sharpened syringe needle (NE-301PL-C; Small Parts, Miramar, FL). The flow layer PDMS

piece was then cleaned and treated with oxygen plasma (PX-250; March Plasma Systems, Concord, CA) for 30 s. It was immediately aligned on the top of the control layer PDMS membrane (still on the silicon wafer) based on alignment marks under a stereomicroscope (SMZ-U, Nikon, Japan) and assembled together to enclose the flow channels. After placing in an oven at 75 °C for 2 h to form an irreversible bond, the PDMS block containing flow and control layers was removed from the control layer silicon template, through-holes were punched at the end of all control channels, and the assembly was finally bonded to an unpatterned PDMS piece to enclose the control channels using oxygen plasma treatment. The final PDMS microdevice was cured in an oven at 120 °C for at least 48 h for complete curing and hydrophobic recovery. Figure 1D shows the droplet extraction interface portion of the PDMS microfluidic device.

2.3 Selective modification of the aqueous channel surface

The aqueous stream flow channel surface was selectively modified to be hydrophilic using corona discharge, while the oil stream flow channel surface retained the hydrophobicity of native PDMS. Deionized water was first gently introduced into the oil flow channel using a syringe through the oil outlet. Due to the hydrophobic PDMS surface and high flow resistance through the small apertures, water was confined to the oil flow channel and a water/air interface was produced at the junction (Figure 1E), leaving the aqueous channel open while protecting the oil flow channel. A corona discharge unit (BD-20AC; Electro-Technic Products, Chicago, IL) with a fine tip electrode was then placed close to the aqueous buffer inlet and actuated for 1–2s. The generated plasma was dispersed into the channel and then water immediately entered into the aqueous channel through the interface, indicating that the aqueous channel surface was oxidized to be hydrophilic. Finally, the water in the oil flow channel was replaced by oil, but the modified aqueous channel surface was kept in the water environment to maintain the modified surface.

2.4 Device operation

Droplet generation in this work was controlled by integrated pneumatic valves, which were actuated by a computer-controlled external solenoid valve as described previously (Sun, 2011a). The valving control channels in the PDMS device were filled with water to avoid introduction of air bubbles into the flow channels. The continuous oil (Fluorinert FC-40, 3M) flow in the channel was controlled by a syringe pump (PHD 2000; Harvard Apparatus, Holliston, MA) through a fused-silica capillary (75 μm i.d., 360 μm o.d.; Polymicro Technologies, Phoenix, AZ). One end of the capillary was connected with a 50 μL syringe (Hamilton, Reno, NV) and the other end was inserted into a ~2 mm long section of Tygon tubing (TGY-101-5C; Small Parts, Miramar, FL) to create a pressure fitting at the oil inlet on the microchip. The dispersed aqueous solutions were stored in sealed vials with a nitrogen gas inlet to pressurize the liquid and an outlet to allow liquid to be transferred into the microchannels via a capillary. Before operation, any air bubbles trapped in the transfer lines and microchannels were removed. The pneumatic valves were actuated to disperse aqueous solutions into the oil flow channel to generate droplets. The continuous aqueous/ESI buffer solution was infused into the aqueous channel from a syringe through a capillary transport line. The infusion rate was controlled by a syringe pump. For experiments in which electroosmotic flow was employed in the aqueous channel, a high voltage was applied over

that channel using a PS-350 high-voltage power supply (Stanford Research Systems, Sunnyvale, CA, USA) via platinum electrodes placed in the reservoirs.

2.5 Detection

A fluorescence detection system was employed to monitor fluorescein-containing droplets (Sun, 2011a). The UV light generated by a mercury lamp (Olympus, Tokyo, Japan) was passed into an inverted optical microscope (Olympus, Tokyo, Japan), and fluorescence was collected with a digital camera (Nikon, Tokyo, Japan). For MS detection, an ion funnel-modified (Kelly, 2010) orthogonal time-of-flight MS instrument (G1969A LC/MSD TOF, Agilent Technologies, Santa Clara, CA) was used. Before coupling with MS, an integrated ESI emitter was created by making two vertical cuts through the PDMS device based on patterned guide lines such that the aqueous channel terminated at the apex (Kelly et al., 2008; Sun et al., 2010). The microfluidic emitter was positioned 3 mm in front of the MS inlet capillary, which was heated to 120 °C. The electrospray potential was applied on the ESI buffer-delivering syringe needle by a high-voltage power supply.

3. Results and discussion

3.1 Droplet extraction interface

Achieving reliable and highly efficient droplet extraction is of great importance for many droplet-based microfluidic systems integrated with further analytical functions such as chemical separations or MS detection. Ideally, each aqueous droplet should be entirely transferred to the aqueous flow channel to avoid losing any important quantitative information. On the other hand, oil should be prevented from entering the aqueous flow channel to avoid negatively impacting the downstream analysis (e.g., blocking flow, interrupting the electrospray circuit or adding chemical background to MS signal). The present droplet extraction interface retains the previously developed geometry of an array of cylindrical posts with narrow apertures in between, but we further strengthened the interface by modifying the aqueous channel to be hydrophilic while the oil flow channel surface remained hydrophobic. Corona discharge was used to treat the aqueous flow channel surface, and the hydrophobic surface in the oil flow channel was prevented from corona exposure by filling the channel with water beforehand. A similar method utilizing corona treatment was reported recently to extract droplets entering the device from a capillary for electrochemical detection (Filla et al., 2011). In the work described here, after actuating the corona discharge for 1–2s, the water entered into the modified channel quickly through the apertures and wetted the oxidized surface, which protected the PDMS surface from recovering its hydrophobicity. The treated device could usually survive for 2–3 days, and repeated surface treatments could likely be applied thereafter (although not explored here). Thus, the channel surfaces on both sides of the interface had different surface energies, which resulted in a very stable aqueous/oil interface established at the junction (Figure 1F).

3.2 Droplet extraction without hydrodynamic aqueous flow

In many of the previously reported systems, an appropriate aqueous stream flow was required to balance the pressure at the interface. In order to test the interface stability of our present device, we first investigated the droplet extraction performance without any

hydrodynamic flow in the aqueous channel. Figure 2 shows the fluorescein droplet transfer at the interface when the oil flow rate was 500 nL/min and there was no flow in the aqueous channel. The entire droplet (~650 pL) was extracted in approximately 100 ms. In contrast to our previous report (Kelly et al., 2009), the droplet transfer occurred through all the apertures. Based on the fluorescence intensity measurement immediately before and after extraction, the droplet content was not significantly diluted during the extraction process. The extracted droplet displaced the aqueous buffer toward the aqueous inlet due to lower resistance, where it remained due to an absence of flow in that channel. To transport the extracted droplet contents, a 500 V/cm electric field was applied over the aqueous channel. The fluorescein molecules migrated at a rate of ~1 mm/s driven by a combination of electrophoresis and electroosmotic flow, which indicated that the effective mobility of fluorecein was approximately 2×10^{-4} $cm^2V^{-1}s^{-1}$ in this case. This arrangement suggests that the droplet transfer event could potentially constitute a novel injection method for an electrophoretic separation. While the possibility is enticing, in the present form the droplet volumes were too large to serve as an efficient CE injection plug. However, utilizing EOF for post-extraction transport is attractive in that the plug-shaped flow profile can help to avoid the band broadening Taylor dispersion associated with pressure-driven laminar flow.

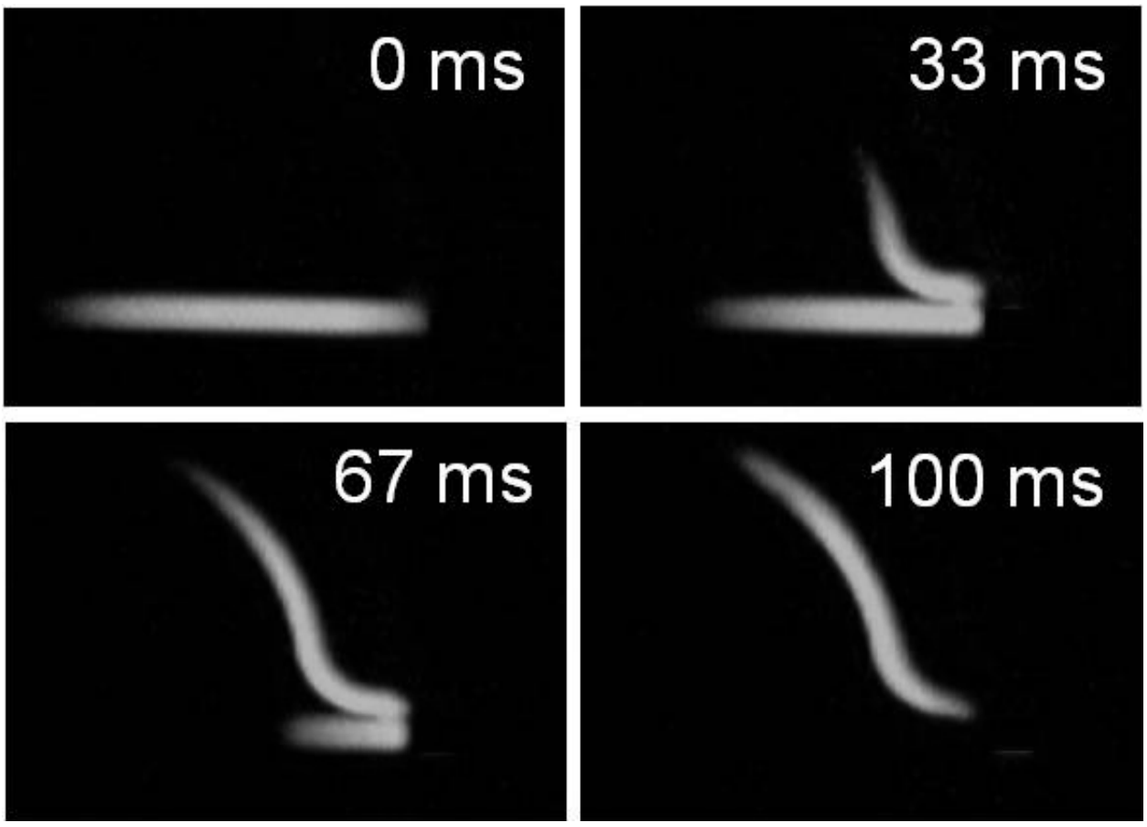

Fig. 2. Micrograph sequences depicting a droplet extraction without pressure-driven flow in the top aqueous channel. The oil phase flow rate was 500 nL/min.

3.3 Impact of oil and aqueous flow rates on droplet extraction

Where EOF-based transport is not practical, hydrodynamic flow is utilized for transport of the extracted contents in the aqueous channel. We showed previously that by positioning the detector sufficiently close to the extraction region, the droplet contents could be analyzed with essentially no dilution (Kelly et al., 2009). However, the flow rates in the oil and aqueous channels needed to be carefully balanced to maintain a stable extraction interface as even a small variance of the aqueous flow rate could disrupt the droplet extraction. The current interface maintained much more robust and effective droplet extraction, enabling the effect of large changes in the aqueous flow rate to be explored. As a baseline, Figure 3A presents a micrograph sequence depicting the droplet extraction procedure in which both the oil and aqueous flow rates were 400 nL/min. When the aqueous plug arrived at the interface, the entire droplet rapidly transferred to the aqueous flow channel. The extracted droplet content was forced to flow in the direction of the hydrodynamic aqueous flow immediately, and the sample stream filled the entire channel cross-section with minimal dilution. Figure 3B shows the droplet transfer behavior at different aqueous flow rates. The oil flow rate was kept constant at 200 nL/min. In each case, the interface was kept stable, and effective droplet transfer was obtained because of the low surface energy and strong capillary force applied on the droplet. When the aqueous flow rate was larger than the oil flow rate, the high pressure originating from the aqueous buffer flow resulted in large resistance to droplet transfer and confined the extracted sample plug into a narrow stream in the aqueous flow channel. Further increasing the aqueous flow rate led to an increase in the droplet transfer (Figure 3C) and a narrowing of the extracted sample stream (Figure 3B), which indicated that the sample would be diluted much more after extraction. When the aqueous flow rate was lower than that in the oil channel, the extraction event essentially disrupted the aqueous flow and the extracted sample inserted itself into the aqueous stream. The excellent stability of the interface enables the oil and aqueous flow rates to be selected independently based upon the desired properties; where dilution should be minimized, it is important that the aqueous flow rate does not exceed that of the oil stream. Varying the oil stream flow rate while holding the aqueous stream constant produced analogous results as shown in Figure 4.

3.4 NanoESI-MS analysis of extracted droplets

The extracted droplet contents could be delivered by the aqueous flow to a monolithically integrated ESI emitter (Kelly et al., 2009; Zhu & Fang, 2010) for MS detection. Figure 5 shows the MS detection of droplets containing 1 μg/μL apomyoglobin in DI water. The oil and ESI buffer flow rates were 100 nL/min and 400 nL/min, respectively. The droplet generation frequency was 0.1 Hz. For a continuous analysis of 60 droplets in 10 min (shown in Figure 5A), the relative standard deviation (RSD) of the peak heights was 3.2%, and RSD of the peak widths was 5.7%. Figure 5B is a zoomed-in view of the MS detection of apomyoglobin droplets in 2 min from the same experiment as shown in Figure 5A. The mass spectrum of peak (a) indicated from Fig. 5B is shown in Fig. 6A with the characteristic signal for the multiply charged protein. Figure 6B shows the mass spectrum of the baseline between two droplets. No protein peaks were observed, which demonstrates there was no cross-contamination between extracted droplets.

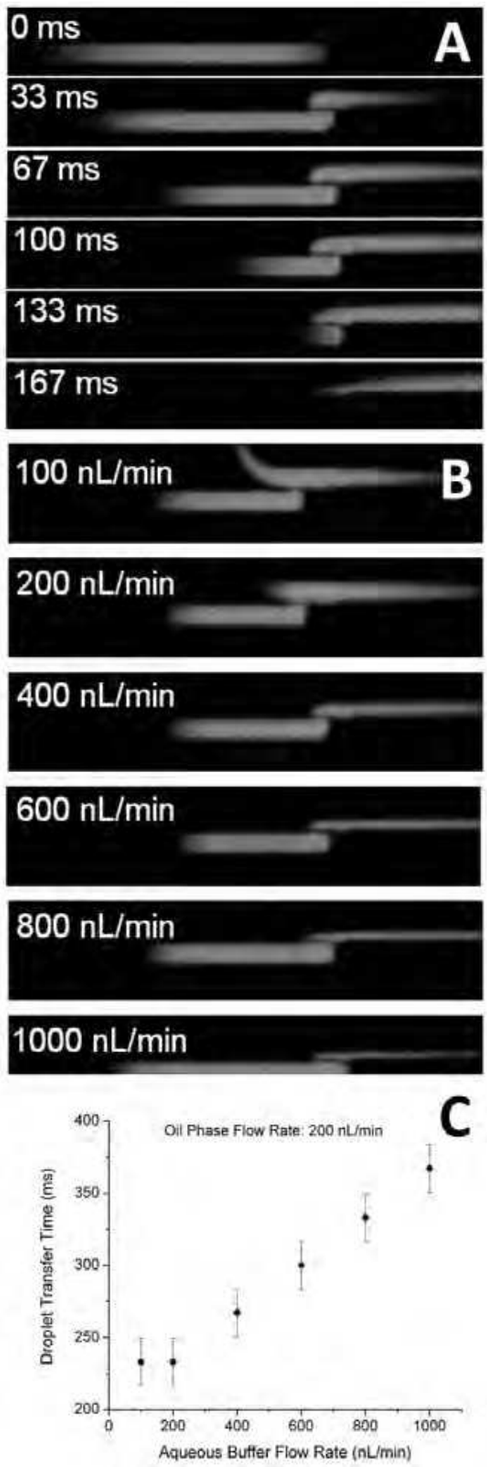

Fig. 3. (A) Micrograph sequence depicting the extraction of an individual fluorescein droplet. The flow rate in both channels was 400 nL/min. (B) Photographs of droplet extraction at different aqueous buffer flow rates. The flow rate of the continuous oil phase was 200 nL/min. (C) Plot of droplet transfer time versus aqueous buffer flow rate.

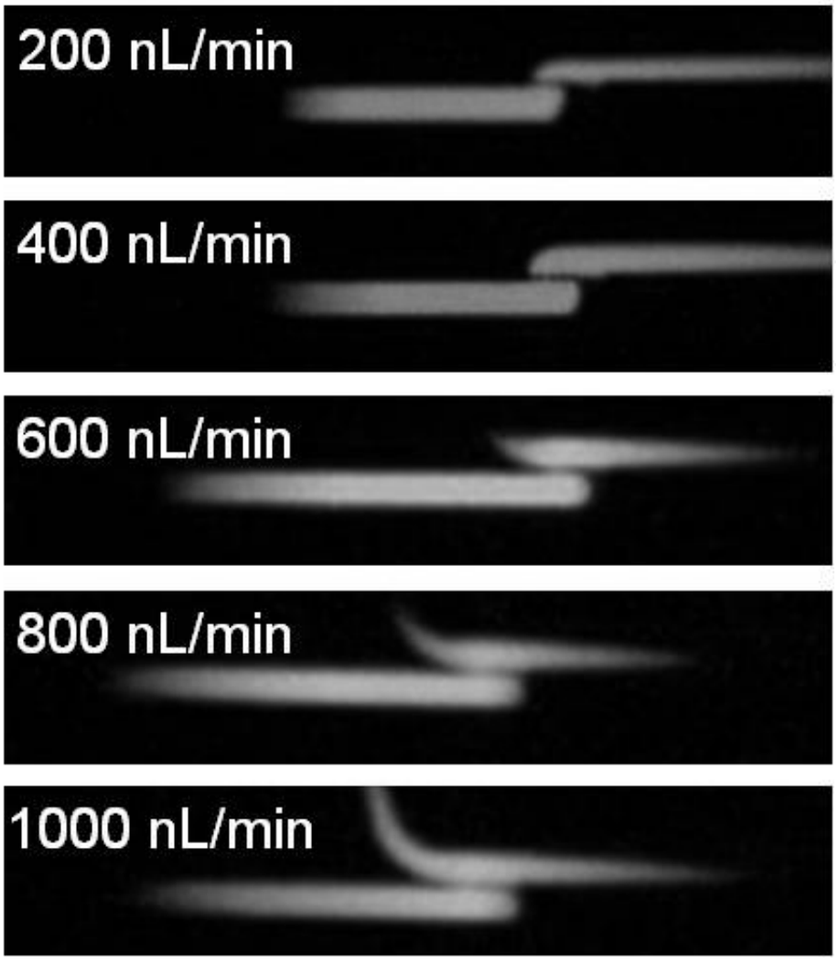

Fig. 4. Photographs of droplet extraction at different oil phase flow rates. The flow rate of the aqueous buffer was 400 nL/min.

The impact of oil and ESI buffer flow rates on MS detection was investigated using 1 μM leucine enkephalin as the aqueous sample. Figure 7A shows the variance of the MS peak intensity and width with ESI buffer flow rate, in which the oil flow rate was kept constant at 100 nL/min. With an increase in the ESI buffer flow rate, both the MS peak intensity and width decreased. This result is consistent with the discussion above, i.e., that the increase in the ESI buffer flow rate would dilute the extracted droplet content much more and broaden the actual sample band. The decrease in peak width is due to the increased flow rate as shown in Figure 3B. In addition, the electrospray ionization efficiency was reduced when increasing the ESI buffer flow rate, which would also influence the MS peak intensity negatively. Figure 7B shows the effect of oil flow rate on MS detection. The ESI buffer flow rate was held constant at 500 nL/min. At lower oil flow rates (< ESI buffer flow rate), the MS peak intensity increased and the peak width decreased with increase in the oil phase flow rate, which resulted from the minimized dilution during droplet extraction. When the oil flow rate increased further (≥ ESI buffer flow rate), the MS peak intensity and width changed less, which was due to the droplet transfer with minimal dilution in these situations.

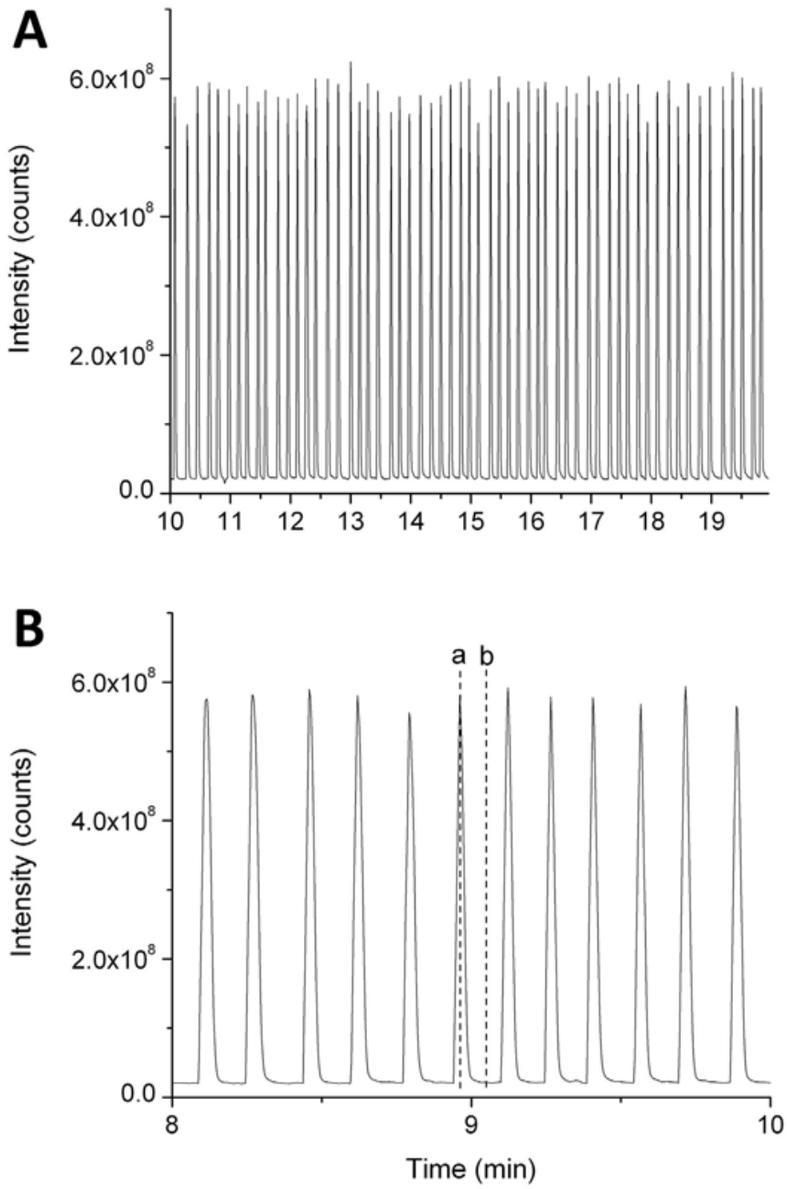

Fig. 5. MS signal intensity (total ion count) vs. time. (A) Detection of the extracted 1 μg/μL apomyoglobin droplets. Oil phase flow rate was 100 nL/min, ESI buffer flow rate was 400 nL/min, and droplet generation frequency was 0.1 Hz. (B) Detailed view of the MS-detected extracted apomyoglobin droplets. (a) and (b) correspond to mass spectra in Fig. 6.

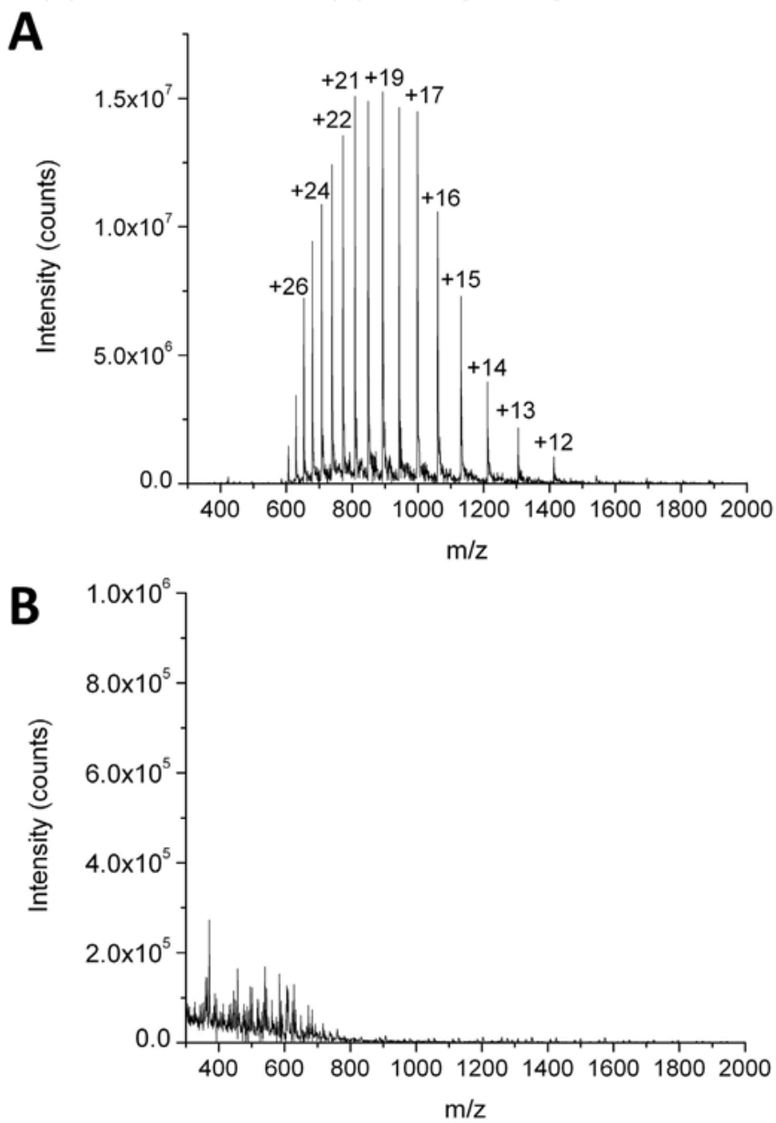

Fig. 6. (A) and (B) Mass spectra obtained from the peak and baseline indicated as (a) and (b) in Fig. 5B, respectively.

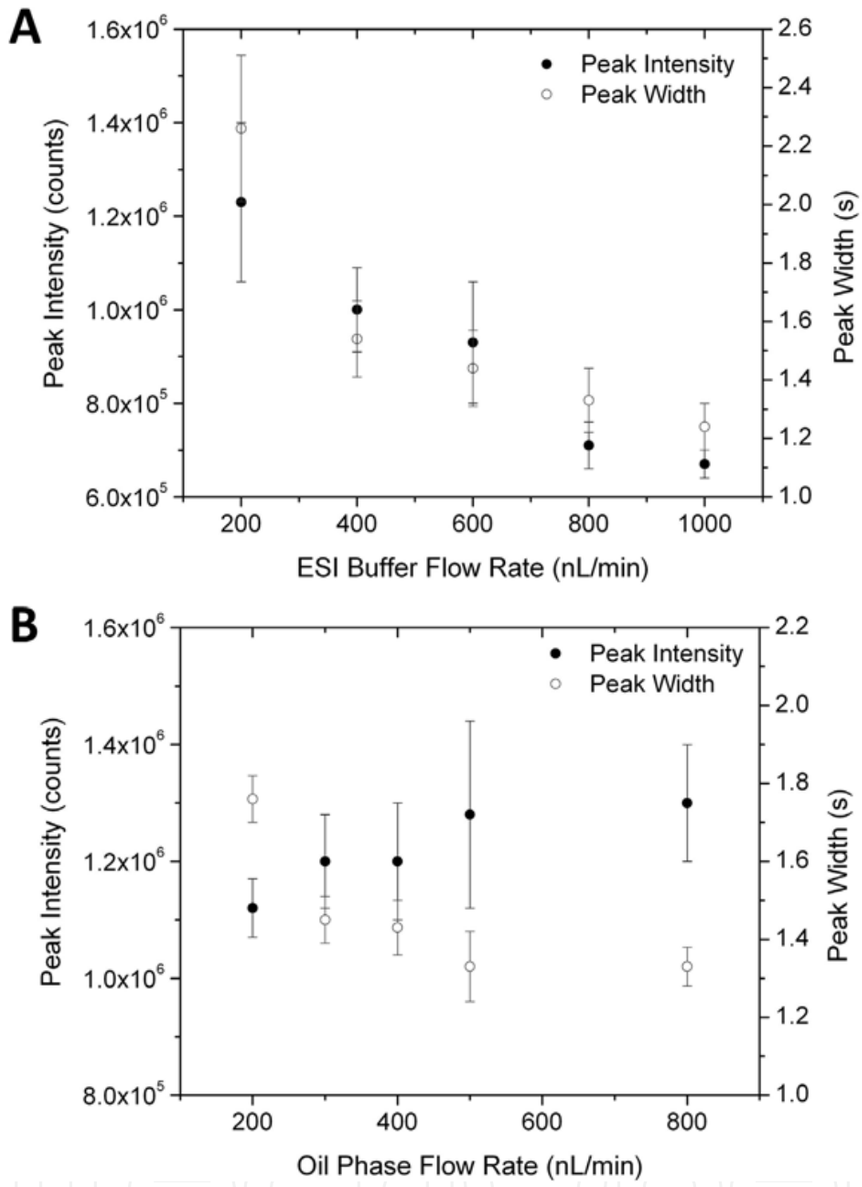

Fig. 7. (A) Plot of MS peak intensity and width vs. ESI buffer flow rate. The sample was 1 μM leucine enkephalin. Oil phase flow rate was 100 nL/min. (B) Plot of the MS peak intensity and width vs. oil phase flow rate. ESI buffer flow rate was 500 nL/min.

4. Conclusion

We developed a robust and efficient droplet extraction interface integrated in a droplet-based PDMS microfluidic device. The interface was constructed with an array of cylindrical posts with small apertures in between. On one side of the interface, the aqueous phase flow channel surface was selectively modified to be hydrophilic by corona discharge. The other side, i.e. the continuous oil phase flow channel surface, remained hydrophobic by protecting the surface with water. The combination of the narrow apertures and surface modification

changed the surface tension at the interface. The lower surface energy of the hydrophilic surface for aqueous droplet and capillary force originated from the small structure facilitated the aqueous droplet transfer while preventing the oil from entering the aqueous flow channel. The resulting surface tension not only helped to establish a stable interface at the junction, but also enabled large pressure imbalances resulting from different oil and aqueous flow rates to be tolerated. All droplets could be transferred through the interface entirely within broad ranges of aqueous flow rates (0 – 1 μL/min, i.e. 0 – 1.33 cm/s) and oil flow rates (100 nL/min – 1 μL/min, i.e. 0.13 – 1.33 cm/s). When the oil flow rate was smaller than the aqueous flow rate, the higher pressure from the aqueous flow slowed the droplet transfer and squeezed the extracted sample stream, which induced dilution of the droplet content after extraction. If the aqueous flow rate was lower, the droplets were extracted rapidly and without dilution. The extracted droplet contents could be analyzed by MS through a monolithically integrated ESI emitter and the droplet extraction efficiency was 100%. The interface described here will form a key component in integrated platforms for reactions and analyses at the picoliter scale.

5. Acknowledgements

Portions of this research were supported by the U.S. Department of Energy (DOE) Office of Biological and Environmental Research, the NIH National Center for Research Resources (RR018522) and the Environmental Molecular Sciences Laboratory (EMSL), a U.S. DOE national scientific user facility located at the Pacific Northwest National Laboratory (PNNL) in Richland, WA. PNNL is a multiprogram national laboratory operated by Battelle for the DOE under Contract No. DE-AC05-76RLO 1830.

6. References

Aebersold, R. & Mann, M. (2003). Mass spectrometry-based proteomics. *Nature*, Vol.422, No.6928, (March 2003), pp. 198-207, ISSN 0028-0836

Chiu, D. T. & Lorenz, R. M. (2009). Chemistry and Biology in Femtoliter and Picoliter Volume Droplets. *Accounts of Chemical Research,* Vol.42, No.5, (May 2009), pp. 649-658, ISSN 0001-4842

Chiu, D. T.; Lorenz, R. M. & Jeffries, G. D. M. (2009). Droplets for ultrasmall-volume analysis. *Analytical Chemistry*, Vol.81, No.13, (July 2009), pp. 5111-5118, ISSN 0003-2700

Fidalgo, L. M.; Whyte, G.; Bratton, D.; Kaminski, C. F.; Abell, C. & Huck, W. T. S. (2008). From microdroplets to microfluidics: selective emulsion separation in microfluidic devices. *Angewandte Chemie International Edition*, Vol.47, No.11, (February 2008), pp. 2072-2075, ISSN 1433-7851

Fidalgo, L. M.; Whyte, G.; Ruotolo, B. T.; Benesch, J. L. P.; Stengel, F.; Abell, C.; Robinson, C. V. & Huck, W. T. S. (2009). Coupling Microdroplet Microreactors with Mass Spectrometry: Reading the Contents of Single Droplets Online. *Angewandte Chemie International Edition*, Vol.48, No.20, (May 2009), pp. 3665-3668, ISSN 1433-7851

Filla, L. A.; Kirkpatrick, D. C. & Martin, R. S. (2011). Use of a corona discharge to selectively pattern a hydrophilic/hydrophobic interface for integrating segmented flow with

microchip electrophoresis and electrochemical detection. *Analytical Chemistry,* Vol.83, No.15, (June 2011), pp. 5996-6003, ISSN 0003-2700

Galas, J. C.; Bartolo, D. & Studer, V. (2009). Active connectors for microfluidic drops on demand. *New Journal of Physics*, Vol.11, (July 2009), pp. 075027, ISSN 1367-2630

Huebner, A.; Sharma, S.; Srisa-Art, M.; Hollfelder, F.; Edel, J. B. & deMello, A. J. (2008), Microdroplets: a sea of applications? *Lab on a Chip,* Vol.8, No.8 (August 2008), pp. 1244-1254, ISSN 1473-0197

Kelly, R. T.; Tang, K.; Irimia, D.; Toner, M. & Smith, R. D. (2008). Elastomeric microchip electrospray emitter for stable cone-jet mode operation in the nanoflow regime. *Analytical Chemistry*, Vol.80, No.10, (May 2008), pp. 3824-3831, ISSN 0003-2700

Kelly, R. T.; Page, J. S.; Marginean, I.; Tang, K. & Smith, R. D. (2009). Dilution-Free Analysis from Picoliter Droplets by Nano-Electrospray Ionization Mass Spectrometry. *Angewandte Chemie International Edition*, Vol.48, No.37, (September 2009), pp. 6832-6835, ISSN 1433-7851

Kelly, R. T.; Tolmachev, A. V.; Page, J. S.; Tang, K. & Smith, R. D. (2010). The ion funnel: Theory, implementations, and applications. *Mass Spectrometry Reviews,* Vol.29, No.2, (March/April 2010), pp. 294-312, ISSN 1098-2787

Koster, S. & Verpoorte, E. (2007). A decade of microfluidic analysis coupled with electrospray mass spectrometry: An overview. *Lab on a Chip*, Vol.7, No.11, (November 2007), pp. 1394-1412, ISSN 1473-0197

Liu, T.; Belov, M. E.; Jaitly, N.; Qian, W.-J. & Smith, R. D. (2007). Accurate mass measurements in proteomics. *Chemical Reviews*, Vol.107, No.8, (August 2007), pp. 3621-3653, ISSN 0009-2665

Mellors, J. S.; Gorbounov, V.; Ramsey, R. S. & Ramsey, J. M. (2008). Fully integrated glass microfluidic device for performing high-efficiency capillary electrophoresis and electrospray ionization mass spectrometry. *Analytical Chemistry*, Vol.80, No.18, (September 2008), pp. 6881-6887, ISSN 0003-2700

Pei, J.; Li, Q.; Lee, M. S.; Valaskovic, G. A. & Kennedy, R. T. (2009). Analysis of samples stored as individual plugs in a capillary by electrospray ionization mass spectrometry. *Analytical Chemistry*, Vol.81, No.15, (August 2009), pp. 6558-6561, ISSN 0003-2700

Pei, J.; Nie, J. & Kennedy, R. T. (2010). Parallel electrophoretic analysis of segmented samples on chip for high-throughput determination of enzyme activities. *Analytical Chemistry*, Vol.82, No.22, (November 2010), pp. 9261-9267, ISSN 0003-2700

Roman, G. T.; Wang, M.; Shultz, K. N.; Jennings, C. & Kennedy, R. T. (2008). Sampling and electrophoretic analysis of segmented flow streams using virtual walls in a microfluidic device. *Analytical Chemistry*, Vol.80, No.21, (November 2008), pp. 8231-8238, ISSN 0003-2700

Song, H.; Chen, D. L. & Ismagilov, R. F. (2006). Reactions in droplets in microfluidic channels. *Angewandte Chemie International Edition*, Vol.45, No.44, (November 2006), pp. 7336-7356, ISSN 1433-7851

Sun, X.; Kelly, R. T.; Tang, K. & Smith, R. D. (2010). Ultrasensitive nanoelectrospray ionization-mass spectrometry using poly(dimethylsiloxane) microchips with

monolithically integrated emitters. *Analyst*, Vol.135, No.9, (September 2010), pp. 2296-2302, ISSN 0003-2654

Sun, X.; Kelly, R. T.; Danielson III, W. F.; Agrawal, N.; Tang, K. & Smith, R. D. (2011a). Hydrodynamic injection with pneumatic valving for microchip electrophoresis with total analyte utilization. *Electrophoresis*, Vol.32, No.13, (June 2011), pp. 1610-1618, ISSN 0173-0835

Sun, X.; Kelly, R. T.; Tang, K. & Smith, R. D. (2011b). Membrane-based emitter for coupling microfluidics with ultrasensitive nanoelectrospray ionization-mass spectrometry. *Analytical Chemistry*, Vol.83, No.14, (July 2011), pp. 5797-5803, ISSN 0003-2700

Teh, S.-Y.; Lin, R.; Hung, L.-H. & Lee, A. P. (2008). Droplet microfluidics. *Lab on a Chip*, Vol.8, No.2, (February 2008), pp. 198-220, ISSN 1473-0197

Theberge, A. B.; Courtois, F.; Schaerli, Y.; Fischlechner, M.; Abell, C.; Hollfelder, F. & Huck, W. T. S. (2010). Microdroplets in microfluidics: An evolving platform for discoveries in chemistry and biology. *Angewandte Chemie International Edition*, Vol.49, No.34, (August 2010), pp. 5846-5868, ISSN 1433-7851

Unger, M. A.; Chou, H.-P.; Thorsen, T.; Scherer, A. & Quake, S. R. (2000). Monolithic Microfabricated Valves and Pumps by Multilayer Soft Lithography. *Science*, Vol.288, No.5463, (April 2000), pp. 113-116, ISSN 0036-8075

Wang, M.; Roman, G. T.; Perry, M. L. & Kennedy, R. T. (2009). Microfluidic chip for high efficiency electrophoretic analysis of segmented flow from a microdialysis probe and in vivo chemical monitoring. *Analytical Chemistry*, Vol.81, No.21, (November 2009), pp. 9072-9078, ISSN 0003-2700

Yang, C.-G.; Xu, Z.-R. & Wang, J.-H. (2010). Manipulation of droplets in microfluidic systems. *Trends in Analytical Chemistry*, Vol.29, No.2, (February 2010), pp. 141-157, ISSN 0165-9936

Zeng, S.; Li, B.; Su, X.; Qin, J. & Lin, B. (2009). Microvalve-actuated precise control of individual droplets in microfluidic devices. *Lab on a Chip*, Vol.9, No.10, (May 2009), pp. 1340-1343, ISSN 1473-0197

Zeng, S.; Pan, X.; Zhang, Q.; Lin, B. & Qin, J. (2011). Electric control of individual droplet breaking and droplet contents extraction. *Analytical Chemistry*, Vol.83, No.6, (March 2011), pp. 2083-2089, ISSN 0003-2700

Zhu, Y. & Fang, Q. (2010). Integrated droplet analysis system with electrospray ionization-mass spectrometry using a hydrophilic tongue-based droplet extraction interface. *Analytical Chemistry*, Vol.82, No.19, (October 2010), pp. 8361-8366, ISSN 0003-2700.

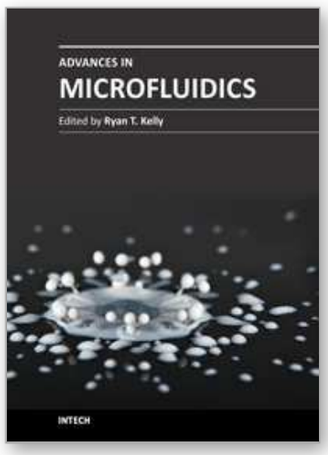

Advances in Microfluidics

Edited by Dr. Ryan Kelly

ISBN 978-953-51-0106-2
Hard cover, 250 pages
Publisher InTech
Published online 07, March, 2012
Published in print edition March, 2012

Advances in Microfluidics provides a current snapshot of the field of microfluidics as it relates to a variety of sub-disciplines. The chapters have been divided into three sections: Fluid Dynamics, Technology, and Applications, although a number of the chapters contain aspects that make them applicable to more than one section. It is hoped that this book will serve as a useful resource for recent entrants to the field as well as for established practitioners.

How to reference

In order to correctly reference this scholarly work, feel free to copy and paste the following:

Xuefei Sun, Keqi Tang, Richard D. Smith and Ryan T. Kelly (2012). Robust Extraction Interface for Coupling Droplet-Based and Continuous Flow Microfluidics, Advances in Microfluidics, Dr. Ryan Kelly (Ed.), ISBN: 978-953-51-0106-2, InTech, Available from: http://www.intechopen.com/books/advances-in-microfluidics/robust-extraction-interface-for-coupling-droplet-based-and-continuous-flow-microfluidics

INTECH
open science | open minds

InTech Europe
University Campus STeP Ri
Slavka Krautzeka 83/A
51000 Rijeka, Croatia
Phone: +385 (51) 770 447
Fax: +385 (51) 686 166
www.intechopen.com

InTech China
Unit 405, Office Block, Hotel Equatorial Shanghai
No.65, Yan An Road (West), Shanghai, 200040, China
中国上海市延安西路65号上海国际贵都大饭店办公楼405单元
Phone: +86-21-62489820
Fax: +86-21-62489821

IntechOpen